1. **TITLE:** Angiopep-2 Grafted PAMAM Dendrimers for the Targeted Delivery of Temozolomide: *In-vitro* and *In-vivo* Effects of PEGylation in the Management of Glioblastoma Multiforme

2. INTRODUCTION

Glioblastoma multiforme (GBM) is the most abundant type of all primary brain tumors of the central nervous system [1]. Based on the profoundness of the disease, glial tumors are classified from grade I (benign) to IV (highly malignant). The benign tumors usually progress into malignant GBM [2]. The primary grade tumors exhibit high infiltrative evolvement characteristics, with the glial tissues travelling apart from the central into the nearby normal brain tissues. Hence, higher-grade glial tumors are more angiogenic and could nurture new leaky blood vessels [3]. As per the report of International Agency for Research on Cancer, approximately 3,08,102 incidences of brain tumor cases were estimated worldwide for the year 2020. Out of which, more than 50% of cases are estimated for Asia (Cancer Today). Approximately 17% of the patients suffering from brain tumor are diagnosed with glioblastoma (Gutkin et al., 2016). Cerebral cortex is mainly affected due to glioblastoma. This includes temporal lobe (31%), parietal lobe (24%), and the frontal lobe (23%) and is rarely found in the brainstem, spinal cord and cerebellum (Shahideh et al., 2012). GBM is one of the deadliest and most aggressive form of brain tumour that is observed in adults.

Due to the presence of blood brain barrier (BBB) and blood brain tumor barrier (BBTB), the majority of the active pharmaceutical moieties cannot reach into the tumor region. The conventional treatment of GBM is deployed on chemotherapy and surgical resection. It is challenging to completely eradicate the pathological cells owing to the invasive growth and unique growth site characteristics of GBM [8]. Radiosensitizers such as nitroimidazoles have been utilized to enhance the sensitivity of hypoxic cells towards chemotherapy radiation. Temozolomide (TMZ) is an FDA approved alkylating agent, which reduces the invasion of tumor cells. TMZ is an established chemotherapeutic agent for treating GBMs due to its penetration to the BBB. It falls under the category of imidazotetrazine. It acts by the methylation of deoxyribonucleoside (DNA) guanine to form O-6-methylguanine [9]. Although TMZ could enhance the possibility of haematological complications like thrombocytopenia, it is vulnerable to fast hydrolysis under physiological conditions, making it difficult to dissolve, and BBB obstruction lowers its anti-glioma efficacy. The other side effects of TMZ involve drug resistance to most gliomas during therapy, fatigue, nausea, and less appetite. TMZ could damage the hematopoietic stem cells due to its DNA methylation property. In the last few

decades, all the above complications with TMZ have been resolved using nanocarriers to deliver TMZ to the target site [10].

Recently, dendrimers have emerged as promising chemotherapeutic delivery tools among many nano drug delivery carriers. Dendrimers are the hyperbranched, multifunctional, and nanosized macromolecules having an core and repetitive external branching units [11]. The branching and multiple functional surfaces of dendrimers bring forth massive sites for ligands and drugs for conjugation. This makes dendrimers a tailor-made nano drug carrier. The diversity of dendrimers has been developed in the last few years with different types, including polyamidoamine (PAMAM), polypropylenimine (PPI), phosphorus (PHH) dendrimers, etc. PAMAM dendrimers have exhibited remarkable results in effective drug delivery to brain by crossing BBB [12]. Previous studies demonstrated that the flexible surface modifications and nanosize of dendrimers could impart the targeting ability of the drug to the glial tumour sites [13]. PEGylation of the nanocarrier have potentially enhanced their brain penetration capabilities [14]. However, the penetration of TMZ to BBB has not been improved effectively and arises an urge to conjugate the dendrimers with specific ligands. The receptor-mediated transcytosis (RMT) process could be initiated by the specific ligands conjugated to nanocarriers and can bind to corresponding receptors overexpressed at BBB prompting the increment of drug accumulation at the site of glioma and drug penetration across the BBB [15].

Peptides have shown excellent outcomes as BBB penetrating ligand. There are several peptides, namely RGD, CREKA, TAT, angiopep-2, etc. which have demonstrated drug targeting efficiency, when conjugated to the surface of nanocarriers [16]. Angiopep-2 (TFFYGGSRGKRNNFKTEEY, molecular weight 2.4 kDa) is extensively used as a specific ligand for lipoprotein receptor-related protein-1 (LRP1). Angiopep-2 belongs to Kunitz domain-derived peptides family and contains high parenchymal accumulation with RMT capacity. According to the previous reports, the nanocarriers functionalized with Angiopep-2 have gained magnificent BBB penetration capability and provide effective targeting delivery of biomolecules to the tumor site [17].

Previously, Ke *et al.* successfully conjugated angiopep-2 to the surface of PEGylated PAMAM dendrimers and utilized the same for gene delivery [17]. However, angiopep-2 anchored PEGylated PAMAM dendrimers have not been explored for TMZ delivery. In the present study, PEGylated and non-PEGylated PAMAM dendrimers were conjugated to Angiopep-2 for the targeted delivery of encapsulated TMZ in the management of GBM **(Figure 1)**. The study aims to facilitate TMZ penetration through BBB and enhance its apoptosis and sensitivity

toward the glioma cells. The study is an attempt to explore the effect of PEGylation and angiopep-2 conjugation to PAMAM dendrimers for better brain delivery of TMZ.

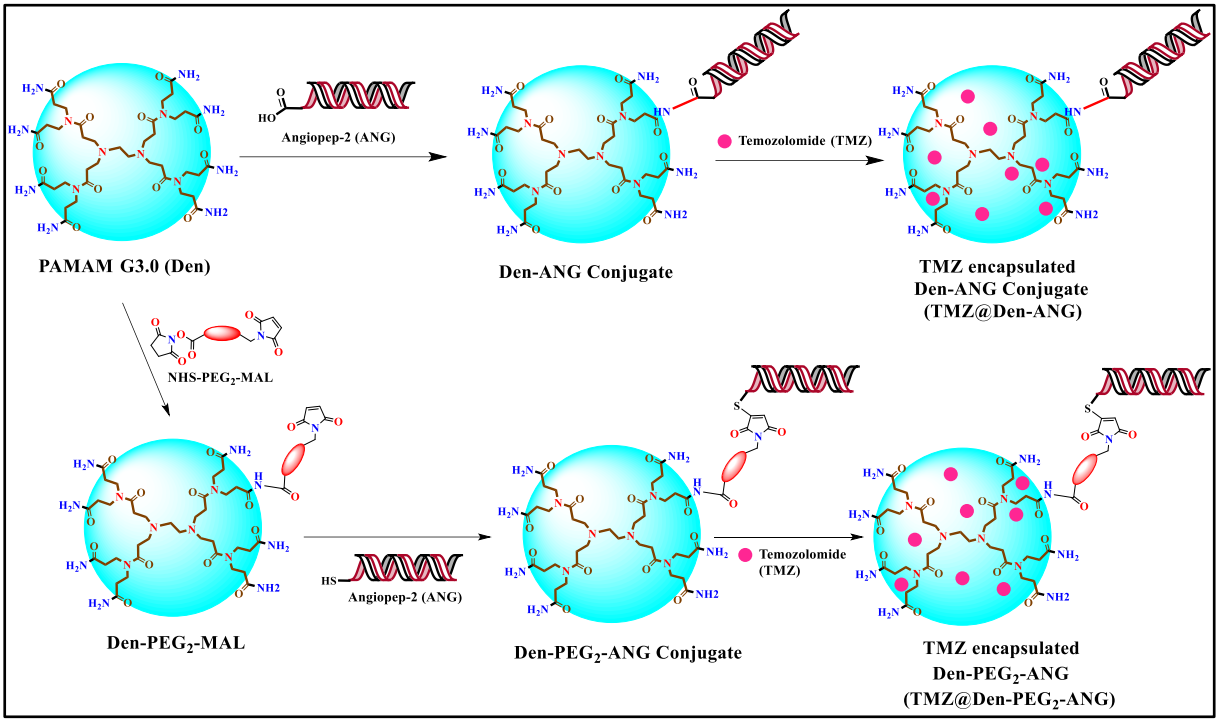

Figure 1: Graphical representation of the preparation of TMZ encapsulated Den-ANG conjugate (TMZ@Den-ANG) and Den-PEG$_2$-ANG conjugate (TMZ@Den-PEG$_2$-ANG)

3. OBJECTIVES

- ✓ To develop a biocompatible dendrimer-based formulation utilizing PEGylation strategy.
- ✓ To improve the pharmacokinetic behavior of TMZ through the novel drug delivery strategy.
- ✓ To enhance the brain penetration of therapeutic moieties through peptide modification approach which should withstand more prone possibility of platform technology in-future for commercialization.

4. MATERIALS AND METHODS

Materials

TMZ and α-malemidyl-ϖ-N-hydroxysuccinimidyl polyethyleneglycol (NHS-PEG$_2$-MAL) was purchased for TCI chemicals, India. Cysteine modified angiopep-2 (TFFYGGSRGKRNNFK TEEYC) was purchased from GenScript, USA. PAMAM dendrimers (G3.0, -NH_2 terminated), dimethyl suberimidate (DMSI), 3-(4,5-dimethylthiazol-2-yl)-2,5-diphenyl tetrazolium bromide (MTT), and fluorescein isothiocyanate (FITC) were purchased from Sigma-Aldrich,

India. Sodium chloride, potassium dihydrogen phosphate, acetone, triethanolamine, and methanol were purchased from CDH, New Delhi, India. Dulbecco's Modified Eagle Medium (DMEM), fetal bovine serum (FBS), phosphate buffer saline pH 7.4 (PBS), and dialysis membrane (5 kDa MWCO) were purchased from HiMedia, Mumbai, India. All the chemicals and reagents were utilized without any further purification and modifications.

Synthesis and Characterization

Den-ANG Conjugate

Cysteine modified angiopep-2 (ANG) was conjugated to the terminal amine groups of PAMAM dendrimers (G3.0) [18] **(Figure 2A)**. Briefly, DMSI was dissolved in triethanolamine HCl buffer (pH 7.4) to which ANG was added and dissolved. Further, PAMAM dendrimers (G3.0) were introduced into the reaction mixture at a molar ratio of 1:4 with ANG. The reaction assembly was kept on stirring for 2 h at room temperature. The product was dialyzed using dialysis membrane (MWCO 5 kDa, HiMedia Laboratories Pvt. Ltd., India) followed by lyophilization to obtain Den-ANG conjugate. To confirm the conjugation, the ^{1}H NMR spectroscopic analysis was performed using Bruker Ascend-500.3MHz, Switzerland. D_2O was used as deuterated solvent for the sample preparation.

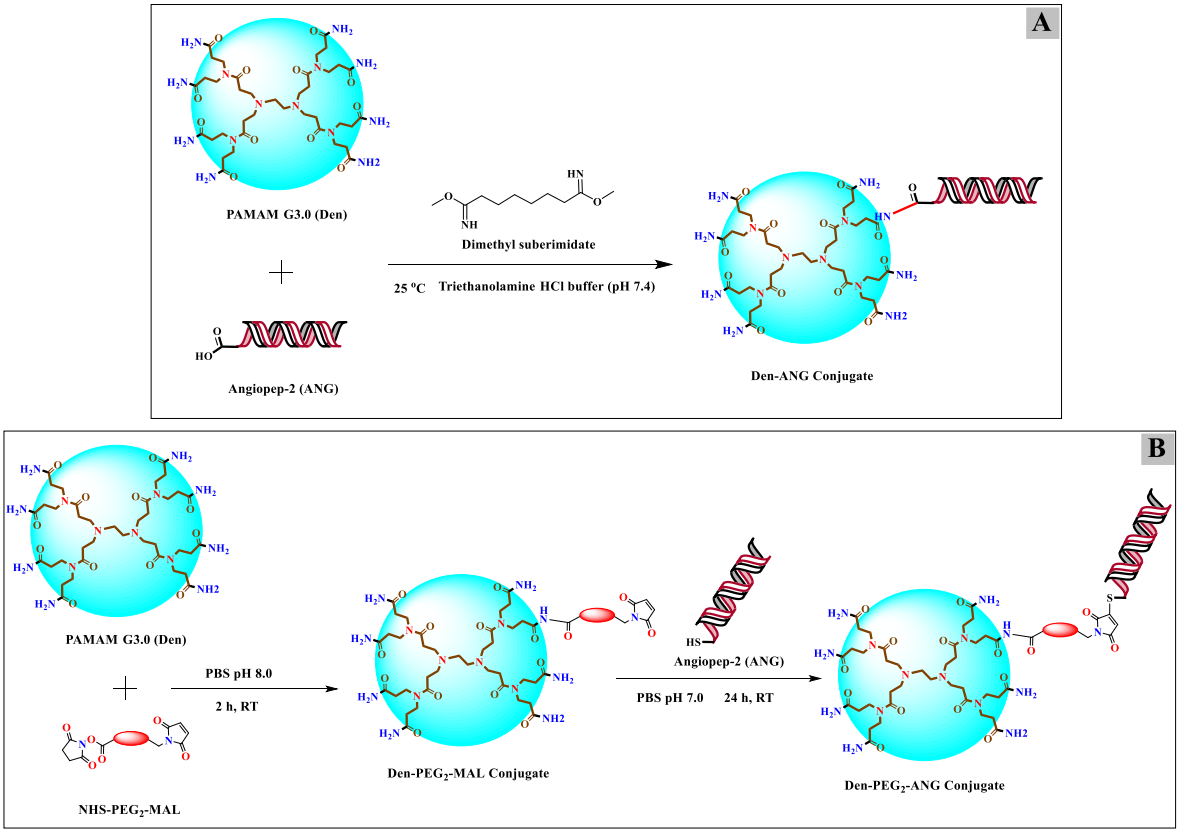

Figure 2: Schematic representation for the synthesis of **A)** Den-ANG conjugate and **B)** Den-PEG_2-ANG conjugate.

Den-PEG$_2$-ANG Conjugate

ANG was conjugated to PEGylated PAMAM dendrimers (G3.0) through a two-step reaction following the previously reported protocol with slight modification [17] **(Figure 2B)**. In the first step, PEGylation was performed and in the second step, ANG was conjugated. Briefly, PAMAM dendrimers (G3.0) were reacted with α-malemidyl-ϖ-N-hydroxysuccinimidyl polyethyleneglycol (NHS-PEG$_2$-MAL) at the molar ratio of 1:2 in phosphate buffer solution (PBS pH 8.0) for 2 h at room temperature. In this step, the terminal NHS group of NHS-PEG$_2$-MAL was conjugated to the peripheral amine groups of PAMAM dendrimers. To purify, the conjugate was dialyzed using dialysis membrane (MWCO 5 kDa, HiMedia Laboratories Pvt. Ltd., India) followed by lyophilization. The obtained Den-PEG$_2$-MAL conjugate was reacted with ANG at a molar ratio 1:1 in PBS pH 7.0 for 24 h at room temperature. The backbone of conjugation was the reaction between thiol groups of Angiopep-2 and MAL group of Den-PEG-MAL conjugate **(Figure 2B)**. The obtained product was dialyzed using dialysis membrane (MWCO 5 kDa, HiMedia Laboratories Pvt. Ltd., India) followed by lyophilization to obtain the purified Den-PEG$_2$-ANG conjugate. To confirm the conjugation, ^{1}H-NMR spectroscopy was performed after each step following the similar procedure as mentioned earlier using D_2O as deuterated solvent.

Atomic Force Microscopy

The three-dimensional (3D) surface of the synthesized conjugates (Den-ANG and Den-PEG$_2$-ANG) were observed using atomic force microscopy (AFM) under ambient conditions [19]. Bruker nanoscope V software was utilized to analyze the surface morphology data of AFM (Bruker, Tapping Mode Co., Germany) to obtain the statistical parameters, like average roughness (Ra), root mean-square roughness (Rq), Kurtosis, and Skewness. Microscopic images of both the conjugates were captured at different scales and analyzed to evaluate the consistency and robustness. The concentration of the prepared samples was 20 μg/mL, out of which only 40−50 μL of the sample was dried on the probe and analyzed. The following parameters were maintained for the microscopic images, i.e., image resolution 256 × 256 pixels, spring constant 40 N/m, and cantilever frequency 300 Hz.

Formulation Development

TMZ encapsulated Den-ANG Conjugate (TMZ@Den-ANG) and Den-PEG$_2$-ANG Conjugate (TMZ@Den-PEG$_2$-ANG)

TMZ was encapsulated into Den-ANG conjugate using previously reported methodology [18]. Briefly, 25 mg of Den-ANG conjugate was dissolved in PBS pH 5.0. Separately, an excess

amount of TMZ was dissolved in PBS pH 5.0 and introduced into the Den-ANG conjugate solution in a dropwise manner. The assembly was kept on magnetic stirring for 24 h to obtain drug loaded formulation i.e., TMZ@Den-ANG.

Similarly, TMZ encapsulated Den-PEG_2-ANG formulation was also developed utilizing 25 mg of Den-PEG_2-ANG conjugate and following the above-mentioned methodology.

HPLC

TMZ was quantified using reverse-phase high-performance liquid chromatography (RP-HPLC) [20]. Shimadzu LC-2010 CHT (M/s Shimadzu Co. Ltd., Chiyoda-ku, Tokyo, Japan) was utilized for the drug estimation, which was well-equipped with RP-18 HPLC column (4.6 × 250 mm, Merck. ODS, particle size 5 µm), autosampler, PDA detector, and LC system. The mobile phase was composed of 0.5% acetic acid solution (AcA) and methanol (MeOH) in a ratio of 10:90 %v/v. The flow rate was maintained by 1.0 mL/min with 25°C maintained column temperature. Each sample was run for 10 min and analyzed at 330 nm wavelength.

Characterization

Particle Size, Zeta Potential, and Polydispersity Index

The particle size, surface charge, and polydispersity index of the developed dendrimeric formulations (TMZ@Den-ANG and TMZ@Den-PEG_2-ANG) were evaluated using Zetasizer (Nano ZS, Version 7.11, Malvern, UK). The lyophilized powders of the developed formulations were dissolved in deionized water of acidic pH and filtered using 0.2 µm syringe filters. The filtered samples were analyzed for the mentioned parameters by DLS technique.

Entrapment Efficiency and Drug Loading

The entrapment efficiency (%EE) and drug loading (%DL) of TMZ@Den-ANG and TMZ@Den-PEG_2-ANG were obtained using membrane dialysis method. The prepared formulations were packed in a dialysis bag (MWCO 5 kDa, HiMedia Laboratories Pvt. Ltd., Bangalore, India) and immersed in 100 mL of PBS pH 5.0 for 2 h. After 2 h, the samples were withdrawn and estimated using RP-HPLC protocol. The %EE and %DL were calculated using the below-mentioned equations.

$$\%\mathrm{EE} = \frac{\text{Total drug} - \text{Amount of untapped drug}}{\text{Total drug}} \times 100$$

$$\%\mathrm{DL} = \frac{\text{Total drug} - \text{Amount of untapped drug}}{\text{Total carrier}} \times 100$$

In-vitro Drug Release

The *in-vitro* drug release studies of pure TMZ, non-PEGylated formulation (TMZ@Den-ANG), and PEGylated formulation (TMZ@Den-PEG_2-ANG) was performed employing the membrane dialysis technique [21]. The drug release profile was observed at both physiological pH (PBS pH 7.4) and acidic microenvironment (PBS pH 5.0). The samples having 2 mg equivalent TMZ were filled in dialysis bags (MWCO 5 kDa, HiMedia Laboratories Pvt. Ltd., India). The sample filled dialysis bags were immersed in 100 mL of PBS and stirred at 150 ± 20 rpm for 72 h 37 ± 2 °C. Further, the 1 mL of samples were withdrawn at specific time intervals while maintaining the sink conditions. The withdrawn samples were then evaluated for TMZ quantification using previously mentioned RP-HPLC protocol. The percent drug release was calculated and plotted with respect to time. The study was performed in triplicate.

Hemolytic Study

The hemolytic assay of pure TMZ, TMZ@Den-ANG, and TMZ@Den-PEG_2-ANG was performed on fresh human blood collected from healthy human volunteer [22]. The collected blood was centrifuged to isolate the RBC pellet. The obtained RBC pellet was washed thrice with 0.9% normal saline solution to remove the plasma and then redispersed in normal saline till use. The samples of 20 ppm drug concentration were prepared using normal saline and RBCs solution was introduced into each sample. The mixture was incubated for 2 h at 37°C. Distilled water was considered as positive control, whereas distilled normal saline was considered as negative control. Then, the incubated samples were centrifuged at 1000 rpm for 10 min (R-4C DX, REMI, India). Further, the supernatant was separated and analyzed at 540 nm using UV-Vis spectrophotometer (Cary series-60, Agilent). The percent hemolysis was calculated by implementing the following formula.

$$\%\, Hemolysis = \frac{Absorbance\ of\ incubated\ samples - Absorbance\ of\ negative\ control}{Absorbance\ of\ positive\ control - Absorbance\ of\ negative\ control} * 100$$

In-vitro Cell-based Studies

Cell Culture (U87MG and LN229 Cells)

U87MG and LN229 glioblastoma cells were grown in T-25 flask using culture media, which was composed of Dulbecco's modified eagle medium (DMEM), fetal bovine serum (FBS), and antibiotic (streptomycin-penicillin) in a ratio of 9:1:0.1, respectively. The flasks containing U87MG cells were incubated in CO_2 incubator (Heracell 150i, Thermo-Fisher) at 37°C temperature and 5% CO_2. When the flask got confluent, the grown cells were trypsinized using

Trypsin-EDTA (0.25% w/v) solution followed by centrifugation to obtain cell pellet. The cell pellet was redispersed in culture media and reused to conduct the mentioned protocols.

MTT Assay

The antitumor activities of pure TMZ, non-PEGylated formulation (TMZ@Den-ANG), and PEGylated formulation (TMZ@Den-PEG_2-ANG) were investigated in U87MG cell lines. MTT assay was performed following a well-established protocol [23]. Cells were seeded in 96-well culture plates maintaining the cell concentration at 10^4 cells per well. The seeded plates were kept for overnight incubation in CO_2 incubator. TMZ have been observed to have IC_{50} values in a wide concentration range. Samples were prepared using the culture media, maintaining the drug concentration up to 200 μM. The seeded 96-well plates were treated with the mentioned formulations of different concentrations followed by incubation. After 24 h, 50 μL of MTT solution were added into each well after PBS washing and further incubated for 4 h. Then, 150 μL of dimethyl sulfoxide (DMSO) was added to each well to dissolve the formazan crystals. Finally, the plates were analyzed for absorbance values at 570 nm using Microplate reader (Omega Fluster, BMG Labtech). Similar procedure was followed for the samples treated for 48 h in U87MG cells. IC_{50} values of each sample were calculated using GraphPad Prism 8.0 software.

Cell Uptake Study

Both PEGylated (TMZ@Den-PEG_2-ANG) and non-PEGylated (TMZ@Den-ANG) formulations were evaluated to measure the qualitative and quantitative cellular uptake in U87MG cells. Briefly, 6-well tissue culture plates were seeded with the U87MG cells uniformly maintaining the cell concentration at 4×10^4 cells per well and incubated overnight. Both the formulations were tagged with fluorescein isothiocyanate (FITC) solution for the qualitative analysis. Briefly, the lyophilized powder of the developed formulation was dissolved in PBS 5.0. Separately, FITC was dissolved in acetone and added to the previously prepared solution. The whole assembly was kept on magnetic stirring for 24 h and dialyzed against PBS to remove the untagged FITC. The cells seeded in 6-well plates were washed using PBS (pH 7.4) prior to FITC tagged formulation treatment. Pure FITC was considered as control. After predetermined time points (24 h and 48 h in separate plates), the culture media was removed from the wells followed by PBS washing. Fluorescence microscopy was performed to evaluate the extent of cellular internalization using fluorescent microscope

(Olympus BS53, Japan). The fluorescence intensity was determined quantitatively using ImageJ software.

Cell Cycle Analysis

To determine the phase of cellular arrest, cell cycle analysis of pure TMZ, TMZ@Den-ANG, and TMZ@Den-PEG_2-ANG were performed using propidium iodide (PI) [24]. The grown U87MG cells were treated with the samples at sub-IC_{50} value, and incubated for the predetermined time (24 h and 48 h separately). After completion of the incubation period, trypsin was added to the treated cells and the detached cells were collected in microcentrifuge tubes. The cell suspensions were centrifuged followed by 1X PBS buffer washing. Chilled ethanol was used for fixing all the samples and incubated in -20°C deep freezer for 3 h. The samples were centrifuged after the incubation period followed by 1X PBS buffer washing. Then, 50 µL of RNase was added to the cells followed by the addition of 50 µL of PI solution after 15 min. The samples were incubated in dark for 20 min. Flow cytometer (BD FACSVerse) was utilized for the estimation cell cycle arrest.

***In-vivo* Studies**

All *in-vivo* experiments were approved by the Institutional Animal Ethics Committee (Approval No. RCPSR/2022/IAEC/21), Rungta College of Pharmaceutical Sciences and Research, Bhilai, Chhattisgarh, India.

Pharmacokinetic Study

The *in-vivo* pharmacokinetic profile of both PEGylated (TMZ@Den-PEG_2-ANG) and non-PEGylated (TMZ@Den-ANG) formulations were evaluated in healthy Sparge-Dawley rats (200-250 g) in comparison to TMZ. 16 healthy rats were utilized for the pharmacokinetic experiment, which were divided into four groups having 4 rats each. The divided groups were administered intravenously with the followings: sterile saline (control), pure TMZ, TMZ@Den-ANG, and TMZ@Den-PEG_2-ANG (5 mg/kg of body weight). After the samples were administered to the rats, blood samples (0.2 mL) were collected from the retro-orbital plexus using heparinized capillary tubes at predefined time points (0.5, 1, 2, 4, 6, 8, 12, and 24 h). The collected samples were centrifuged to remove plasma and stored in acidic environment with deep freezing facility till further use. TMZ plasma content of the collected samples were analyzed through previously mentioned RP-HPLC protocol. 0.5% acetic acid solution (AcA) and methanol (MeOH) in a ratio of 10:90 %v/v was utilized as the mobile phase. The results were further analyzed to determine different pharmacokinetic parameters using PKSolver software.

Bio-distribution Study

Categorization of the selected rats and dosing of TMZ and formulations were kept similar as mentioned in the pharmacokinetic study. The divided groups were administered with the followings: saline water (control), pure TMZ, TMZ@Den-ANG, and TMZ@Den-PEG_2-ANG (5 mg/kg of body weight). Post administration of doses, one rat from each group was sacrificed and the vital organs, such as brain, heart, lungs, kidney, liver, and spleen were removed and homogenized. The homogenized samples of the collected organs were deproteinized followed by centrifugation and filtration. TMZ content in each organ was quantified using previously described RP-HPLC protocol. The data obtained were graphically represented in terms of ng of TMZ content per g of organ/tissue.

5. RESULTS

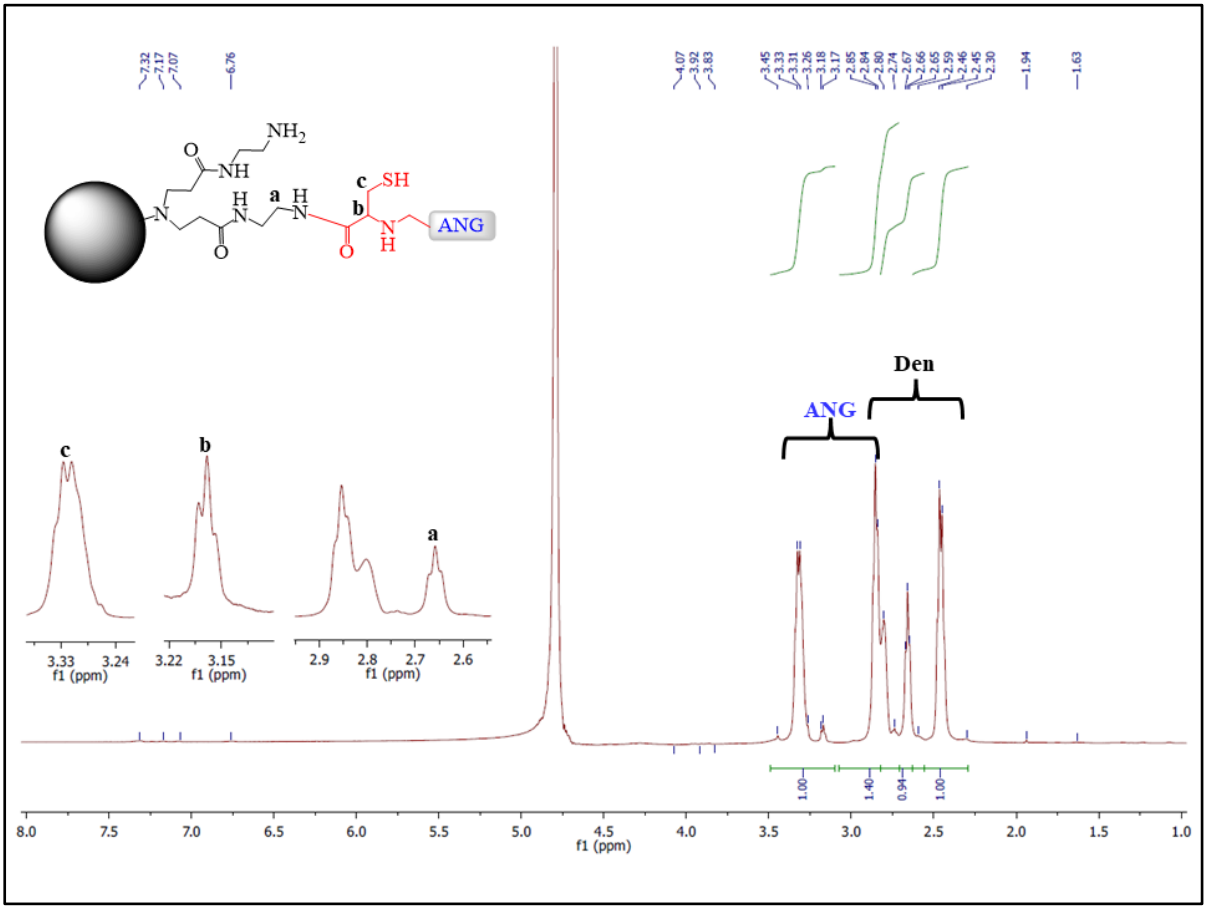

Figure 3: ^{1}H NMR spectra of Den-ANG conjugates.

Synthesis and Characterization of Den-ANG and Den-PEG_2-ANG Conjugate

^{1}H NMR Spectroscopy

The synthesized Den-ANG conjugates were characterized using ^{1}H NMR spectroscopy (500 MHz, Bruker, Switzerland), in which D_2O was used as solvent **(Figure 3)**. The characteristic

peaks were observed at 2.65 ppm (a, triplet, -CH_2 group), 3.20 ppm (b, triplet, -CH_2 group), and 3.33 ppm (c, triplet, -CH_2 group). The characteristic peaks of PAMAM were observed in the range of 2.3 to 3.0 ppm. The obtained NMR data confirmed the synthesis of Den-ANG conjugate.

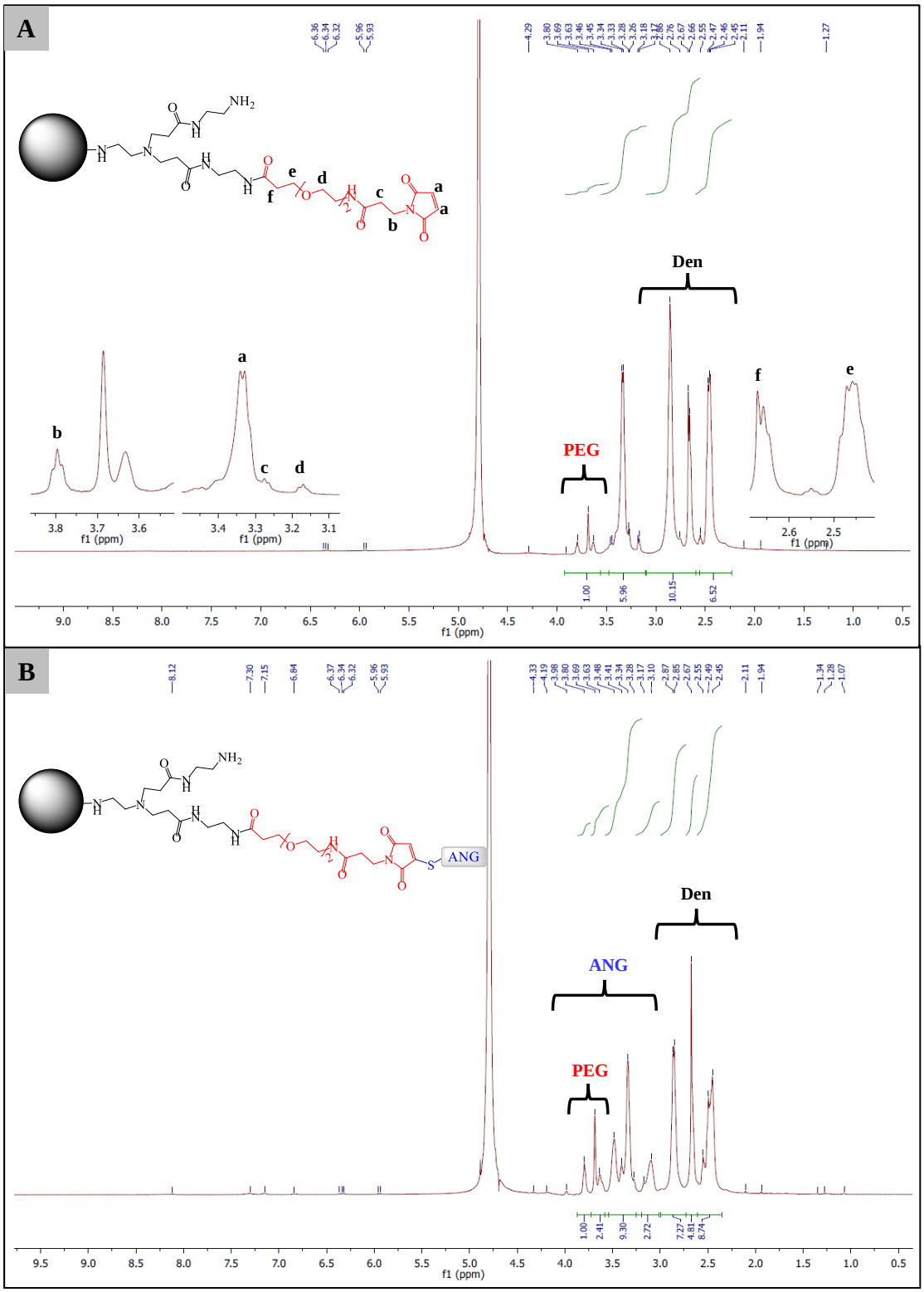

Figure 4: ^{1}H NMR spectra of **A)** Den-PEG_2-MAL and **B)** Den-PEG_2-ANG conjugates.

The synthesized Den-PEG_2-MAL conjugates and Den-PEG_2-ANG conjugates were characterized using ^1H NMR spectroscopy (500 MHz, Bruker, Switzerland). In case of Den-PEG_2-MAL conjugates, D_2O was used as solvent. As depicted in **figure 4A**, the characteristic peaks of PAMAM dendrimers were observed in the range of 2.3 to 3.0 ppm, whereas PEG peaks were observed in the range of 3.5 to 4.0 ppm. Additionally, characteristic peaks were observed at 3.35 ppm (a, doublet, -CH group), 3.8 ppm (b, triplet, -CH_2 group), and 3.27 ppm (c, triplet, -CH_2 group). These findings confirmed the synthesis of Den-PEG_2-MAL conjugates.

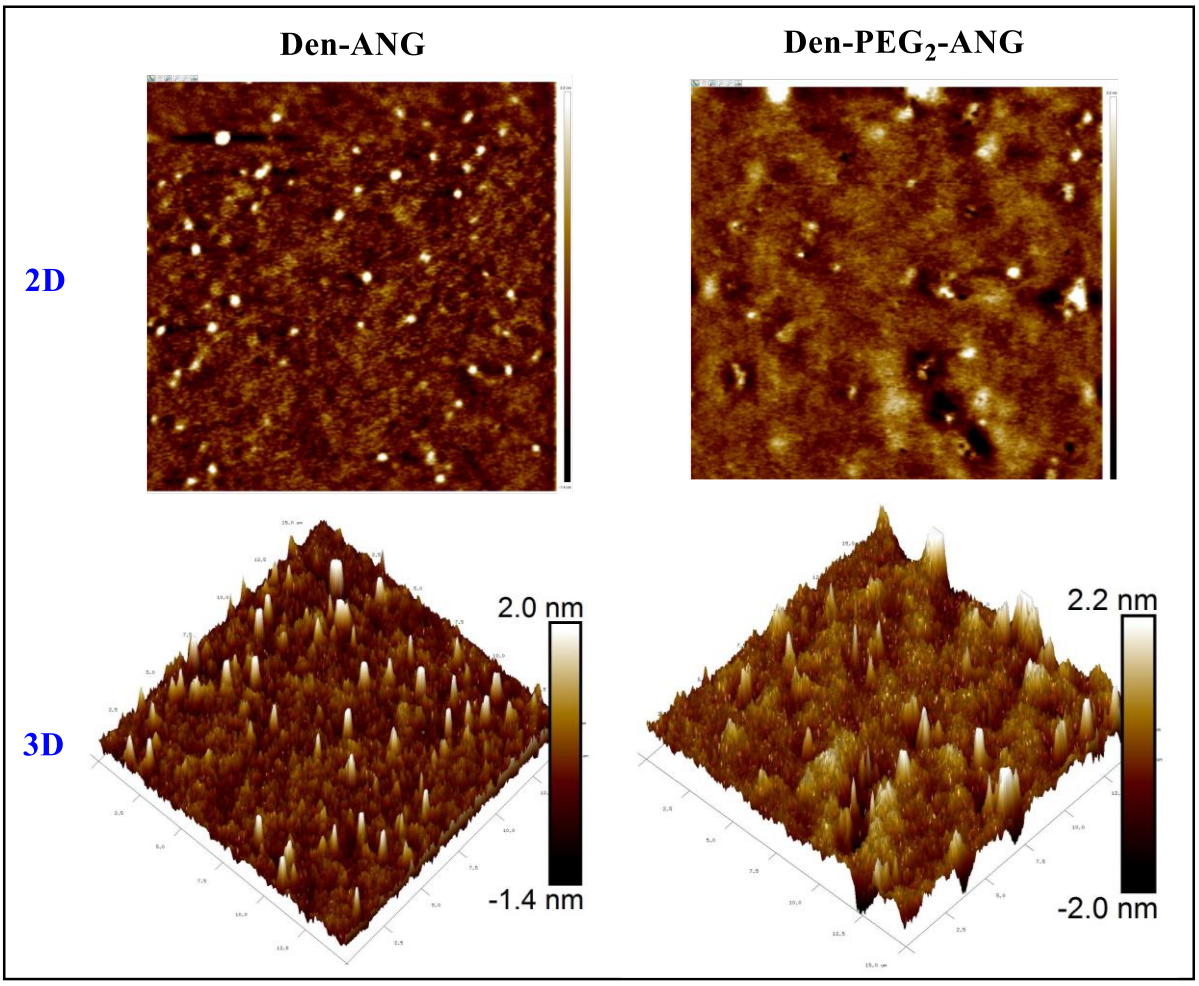

Figure 5: Atomic force microscopic 2D and 3D images of Den-ANG and Den-PEG_2-ANG conjugates (pixels = 256 × 256, spring constant = 40 N/m, and cantilever frequency = 300 Hz).

Atomic Force Microscopy

AFM results revealed that the root-mean-square roughness (Rq) of the synthesized conjugates i.e., Den-ANG and Den-PEG_2-MAL were found to be 0.466 and 0.492 nm, respectively **(Figure 5)**. The surface roughness (Ra) of Den-ANG and Den-PEG_2-ANG conjugates were found to be 0.297 and 0.343 nm, respectively. The Kurtosis and Skewness values of Den-ANG

conjugate were 5.27 and 98.8, respectively. However, the Kurtosis and Skewness values of Den-PEG_2-ANG conjugate were 0.282 and 10.5, respectively.

Formulation Characterization

Particle Size, Zeta Potential, and Polydispersity Index

As depicted in **table 1,** the particle size of the TMZ@Den-ANG and TMZ@Den-PEG_2-ANG was observed to be 229.0 ± 17.8 and 249.6 ± 12.9 nm, respectively. The PDI values of both the formulations were less than 0.4. The zeta potential of TMZ@Den-ANG was found to be 9.06 ± 0.4 mV, whereas the same of TMZ@Den-PEG_2-ANG was found to be 10.9 ± 0.6 mV.

Table 1: Particle size, zeta potential, PDI, percent entrapment efficiency, and percent drug loading of TMZ@Den-ANG and TMZ@Den-PEG_2-ANG. Values represent mean ± SD (n = 3).

Parameter	TMZ@Den-ANG	TMZ@Den-PEG_2-ANG
Particle size (nm)	229.0 ± 17.8	249.6 ± 12.9
Zeta potential (mV)	9.06 ± 0.4	10.9 ± 0.6
PDI	0.311 ± 0.02	0.244 ± 0.03
% Entrapment Efficiency	63.27 ± 5.1	71.48 ± 4.3
% Drug Loading	35.69 ± 2.3	42.97 ± 3.7

Entrapment Efficiency and Drug Loading

The entrapment efficiency of non-PEGylated (TMZ@Den-ANG) and PEGylated (TMZ@Den-PEG_2-ANG) were found to be 63.27 ± 5.1% and 71.48 ± 4.3%, respectively **(Table 1)**. The drug loading of TMZ@Den-ANG and TMZ@Den-PEG_2-ANG were calculated to be 35.69 ± 2.3% and 42.97 ± 3.7%, respectively.

***In-vitro* Drug Release**

The *in-vitro* release behavior of free TMZ, TMZ@Den-ANG, and TMZ@Den-PEG_2-ANG was evaluated in acidic pH (PBS pH 5.0) to mimic the tumor microenvironment. Pure drug was almost completely released within 8 h **(Figure 6A)**. More than 50% of the pure drug was released from TMZ@Den-ANG within 8 h, whereas TMZ@Den-PEG_2-ANG released less than 40% of drug within the same time. After 72 h, TMZ@Den-ANG released more than 90% of the drug, while only 80% of the drug was released from the PEGylated formulation i.e., TMZ@Den-PEG_2-ANG. When the obtained results were fit into different kinetic models, it was found that both TMZ@Den-ANG was best fit in Korsmeyer-Peppas model (R^2 = 0.9796) and first order model (R^2 = 0.9505). However, the release pattern of TMZ@Den-PEG_2-ANG

was best fit in Higuchi model (R^2 = 0.9621), Korsmeyer-Peppas model (R^2 = 0.9484), and first order model (0.9347). In case of PBS pH 7.4, the pure drug was released completely within 8 h, whereas the non-PEGylated (TMZ@Den-ANG) and PEGylated formulations (TMZ@Den-PEG_2-ANG) took 12 h for the complete release of the drug **(Supporting information, Figure S3)**. However, the release profile showed the maximum percent drug release up to 50% only. This may be due to hydrolysis of the drug in basic pH.

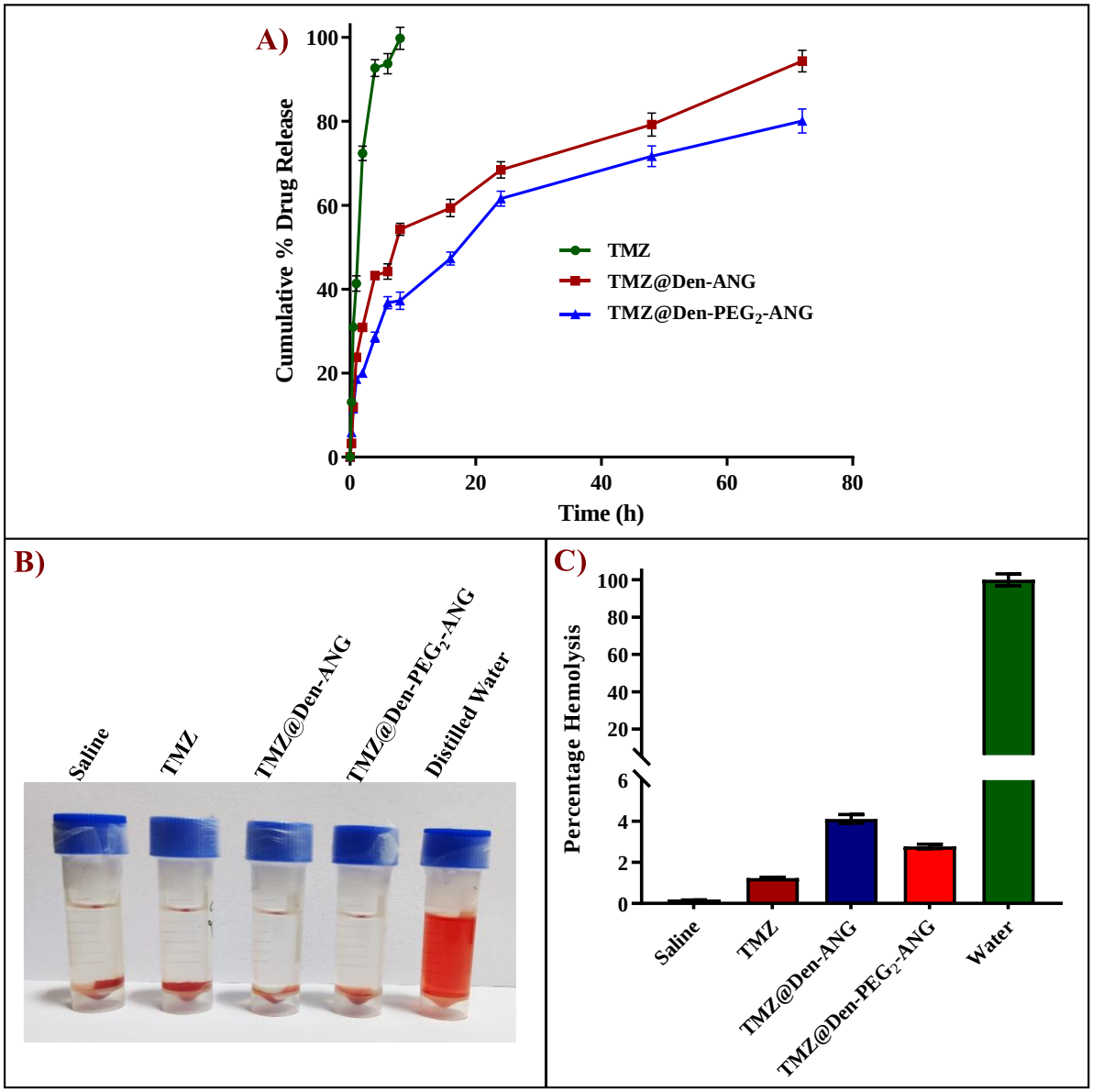

Figure 6: A) *In-vitro* drug release profiles of pure TMZ, TMZ@Den-ANG, and TMZ@Den-PEG_2-ANG in PBS pH 5.0, **B)** picture representing hemolytic effect and **C)** percentage hemolysis of pure TMZ, TMZ@Den-ANG, and TMZ@Den-PEG_2-ANG. Values represent mean ± SD (n = 3).

Hemolytic Assay

The biocompatibility of TMZ, TMZ@Den-ANG, and TMZ@Den-PEG_2-ANG was evaluated through the interaction of the samples with RBCs **(Figure 6B)**. The positive control (distilled water) exhibited complete hemolysis, whereas the negative control (saline) showed almost negligible hemolytic effect. At 20 PPM concentration, free TMZ showed 1.23 ± 0.05% hemolysis. However, ANG grafted drug loaded formulations, namely TMZ@Den-ANG and TMZ@Den-PEG_2-ANG showed 4.12 ± 0.2% and 2.78 ± 0.1% hemolysis, respectively **(Figure 6C)**.

MTT Assay

The cytotoxic effect of free TMZ, TMZ@Den-ANG, and TMZ@Den-PEG_2-ANG was investigated in U87MG glioblastoma cells. The cellular inhibition efficiency of the treated samples was analyzed in the range of 20 to 200 µM TMZ concentration. After 24 h of treatment, free TMZ showed approximately 40% inhibition even at 200 µM concentration. However, TMZ@Den-ANG and TMZ@Den-PEG_2-ANG showed more than 90% inhibition of U87MG cells in the same treatment period **(Figure 7A)**. After 24 h, the IC_{50} values of pure TMZ, TMZ@Den-ANG, and TMZ@Den-PEG_2-ANG were calculated to be 238.09 ± 27.91 µM, 122.74 ± 15.24 µM, and 106.62 ± 11.43 µM, respectively **(Figure 7B)**. In comparison to pure TMZ, the IC_{50} values of TMZ@Den-ANG and TMZ@Den-PEG_2-ANG were reduced by 1.94 and 2.23 folds, respectively.

After 48 h of treatment, TMZ exhibited more than 85% inhibition at 200 µM concentration. Concentration dependent U87MG inhibition was also observed in the treated samples after 48 h treatment **(Figure 7C)**. However, the findings of 48 h were similar to 24 h treatment in case of both TMZ@Den-ANG and TMZ@Den-PEG_2-ANG. After 48 h, the IC_{50} values of pure TMZ, TMZ@Den-ANG, and TMZ@Den-PEG_2-ANG were calculated to be 116.75 ± 10.62 µM, 102.17 ± 8.25 µM, and 85.90 ± 9.12 µM, respectively **(Figure 7D)**. The results revealed that the IC_{50} value of TMZ@Den-ANG was reduced by 1.14 times with respect to free TMZ, whereas the IC_{50} value of TMZ@Den-PEG_2-ANG were reduced by 1.36 times.

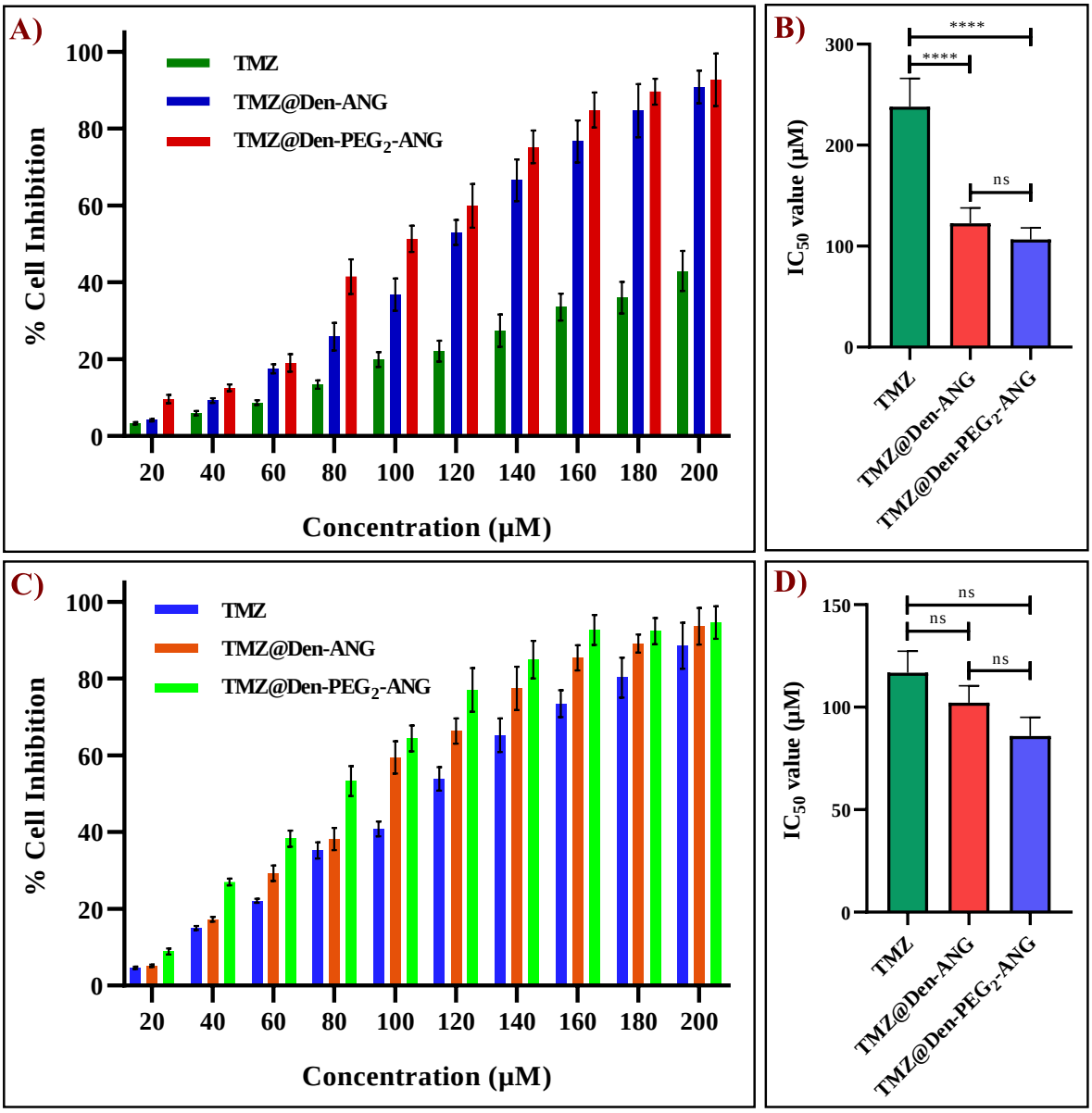

Figure 7: Cytotoxic effects of pure TMZ, TMZ@Den-ANG, and TMZ@Den-PEG_2-ANG against U87MG cells after **A)** 24 h treatment along with the **B)** IC_{50} values and **C)** 48 h treatment along with the **D)** IC_{50} values. **** and ns (not significant) signify $p < 0.0001$ and $p > 0.05$, respectively. Values represent mean ± SD (n = 3).

Cell Uptake Study

The qualitative cellular uptake in U87MG cells was estimated using FITC-labeled TMZ@Den-ANG and TMZ@Den-PEG2-ANG formulations. The fluorescent images were captured at two different time points (24 h and 48 h) using fluorescent microscope (Olympus BS53, Japan) **(Figure 8A)**. No significant cellular uptake was observed in the case of pure FITC even after 48 h of treatment. TMZ@Den-PEG_2-ANG exhibited significantly higher cellular uptake than

TMZ@Den-ANG after 24 h of treatment. Similar results were obtained after 48 h of treatment. However, TMZ@Den-PEG$_2$-ANG exhibited relatively low fluorescence intensity in 48 h post-treatment image than 24 h image.

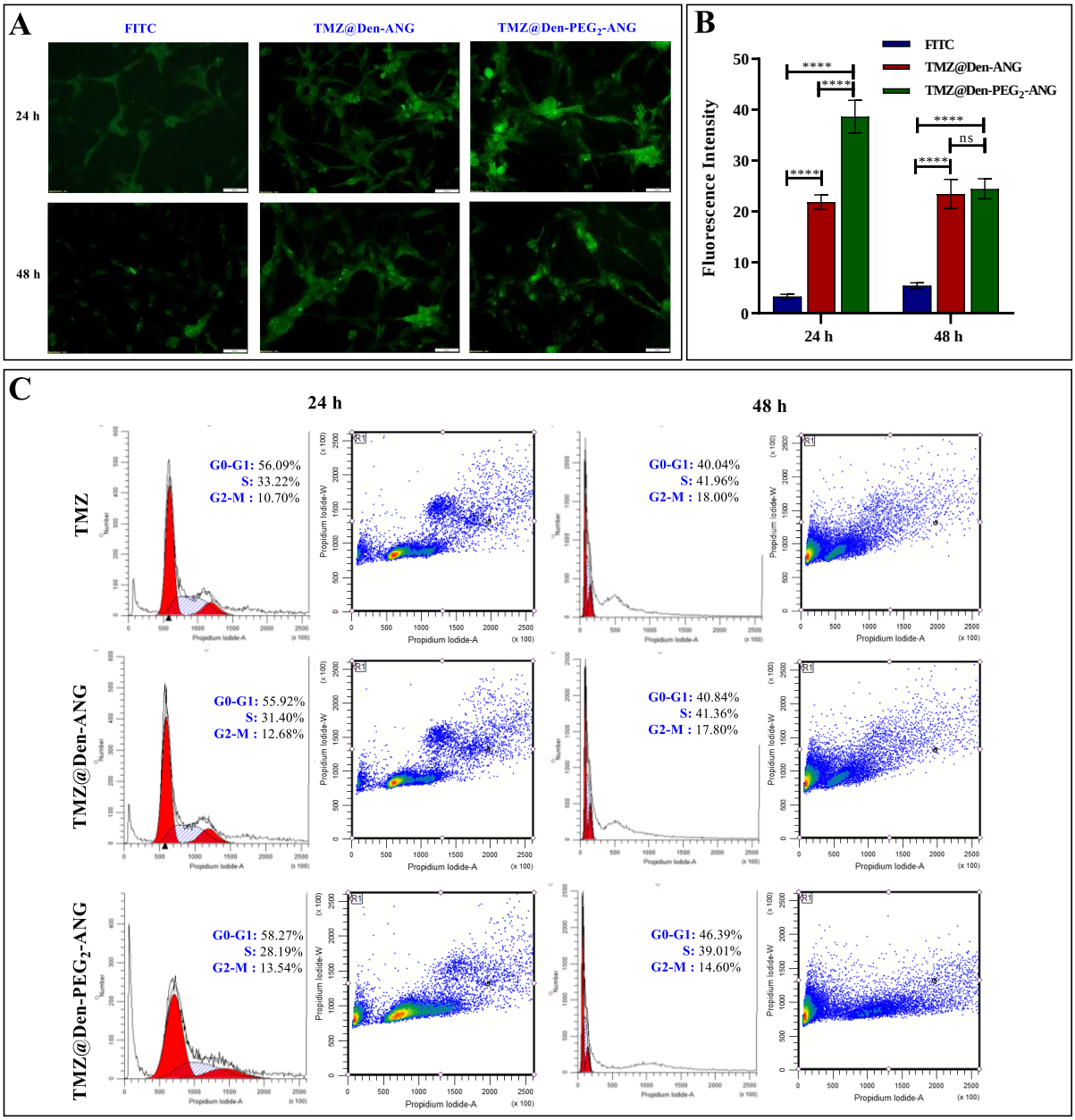

Figure 8: A) Cell uptake study with **B)** quantitative fluorescence intensity estimation using ImageJ software, and **C)** cell cycle analysis of TMZ and the developed formulations (TMZ@Den-ANG and TMZ@Den-PEG$_2$-ANG) in U87MG cells. **** and ns (not significant) signify $p < 0.0001$ and $p > 0.05$, respectively. Values represent mean ± SD (n = 3).

The quantitative estimation of fluorescence intensity also supported the qualitative cellular uptake analysis **(Figure 8B)**. The control group exhibited very low intensity at both 24 h (3.24 ± 0.48) and 48 h (5.35 ± 0.61). The fluorescence intensity was recorded to be 21.84 ±

1.45 in case of non-PEGylated formulation (Den-PEG_2-ANG). Increasing the treatment period to 48 h resulted in enhancement (ns, $p > 0.05$) in fluorescence intensity (23.45 ± 2.87). In case of PEGylated formulation, the fluorescence intensity was observed to be 38.66 ± 3.21 after 24 h. However, the fluorescence intensity decreased significantly ($p < 0.0001$) after increasing the treatment period to 48 h (24.45 ± 1.98).

Cell Cycle Analysis

The cell cycle analysis was performed to determine the phase at which the formulations halt the U87MG cell cycle. As depicted in **figure 8C**, TMZ@Den-ANG halted the cell cycle at G0-G1: 55.92%, S: 31.40%; and G2/M: 12.68%, which is similar to the results of TMZ treated cells after 24 h. Similar findings were obtained in case of TMZ@Den-PEG_2-ANG (G0-G1: 58.27%, S: 28.19%; and G2/M: 13.54%) after 24 h of treatment. However, TMZ@Den-ANG halted the cell cycle at S-phase (41.36%) with G2/M phase inhibition (17.80%). TMZ@Den-PEG_2-ANG also halted the cell cycle at S-phase (39.01%) with 14.60% G2/M phase inhibition.

Pharmacokinetic Study

The pharmacokinetic profiles of TMZ@Den-ANG and TMZ@Den-PEG_2-ANG were plotted analyzed with respect to TMZ **(Figure 9)**. All the animals (Sprague-Dawley rats) survived after the experimental procedure of *in-vivo* pharmacokinetic studies, which suggests 100% survival in all the groups. The plasma concentration of free TMZ was reduced to almost zero within 8 h after the intravenous administration. However, TMZ@Den-ANG and TMZ@Den-PEG_2-ANG exhibited slow *in-vivo* drug release which was monitored up to 24 h.

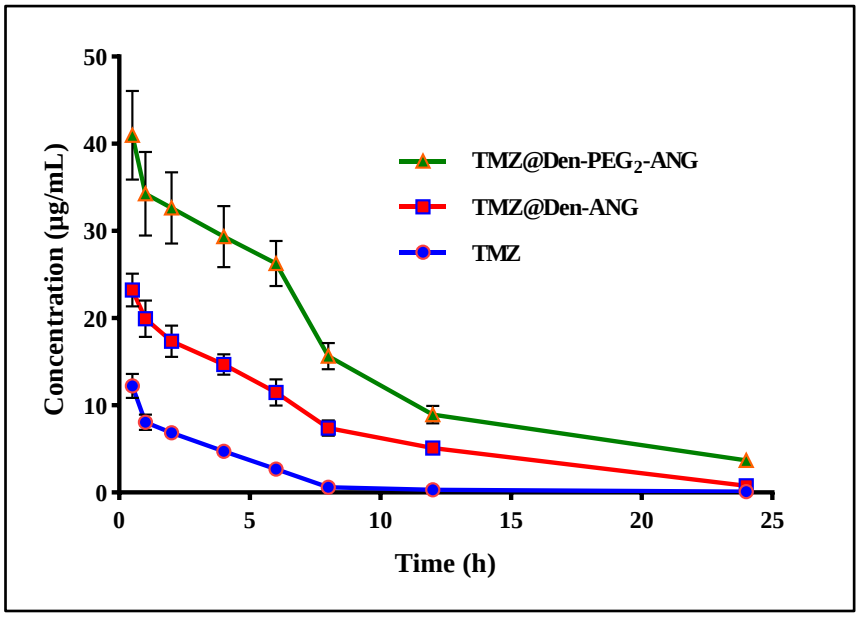

Figure 9: Plasma concentration versus time profile of TMZ, TMZ@Den-ANG, and TMZ@Den-PEG_2-ANG in healthy Sprague-dawley rats. Values represent mean ± SD (n = 4).

Pharmacokinetic parameters were calculated using 1 CBM *i.v.* push model by PKSolver software and listed in **table 2**. The outcomes of the pharmacokinetic study revealed that the bioavailability ($AUC_{0-\infty}$) of TMZ@Den-ANG and TMZ@Den-PEG_2-ANG was enhanced by 4.11 and 8.96 times, respectively in comparison to pure TMZ. The half-life ($t_{1/2}$) values of TMZ@Den-ANG and TMZ@Den-PEG_2-ANG were also enhanced by 2.22 and 2.76 times, respectively, than the pure TMZ. In comparison to pure TMZ, the mean residence time (MRT) values were increased from 3.42 ± 0.40 h to 7.57 ± 0.69 h and 9.44 ± 0.82 h for TMZ@Den-ANG and TMZ@Den-PEG_2-ANG, respectively. The volume of distribution (V_d) was reduced by 1.86 times in case of TMZ@Den-ANG, whereas the value was reduced by 3.25 times in case of TMZ@Den-PEG_2-ANG. The clearance (Cl) values were decrease from 22.85 ± 0.4 mL/h to 5.57 ± 0.41 mL/h for TMZ@Den-ANG and 2.55 ± 0.19 mL/h for TMZ@Den-PEG_2-ANG over the pure drug.

Table 2: Pharmacokinetic parameters obtained from plasma concentration-time profile[#]. **** signifies $p < 0.0001$. Values represent mean ± SD (n = 4).

Parameters	Units	TMZ	TMZ@Den-ANG	TMZ@Den-PEG_2-ANG
AUC_{0-t}	$\mu g.mL^{-1}.h$	43.72 ± 5.91	172.16 ± 20.56****	361.19 ± 28.41****
$AUC_{0-\infty}$	$\mu g.mL^{-1}.h$	43.76 ± 4.86	179.70 ± 16.97****	392.05 ± 33.24****
k	h^{-1}	0.29 ± 0.04	0.13 ± 0.02	0.11 ± 0.01
$t_{1/2}$	h	2.37 ± 0.21	5.25 ± 0.61	6.55 ± 0.43
MRT	h	3.42 ± 0.40	7.57 ± 0.69	9.44 ± 0.82
V_d	L	0.078 ± 0.004	0.042 ± 0.005	0.024 ± 0.003
Cl	mL/h	22.85 ± 0.4	5.57 ± 0.41	2.55 ± 0.19

[#]$AUC_{0-\infty}$ denotes the area under curve (bioavailability), k denotes elimination rate constant, $t_{1/2}$ denotes the half-life, MRT denotes mean residence time, V_d denotes volume of distribution, and Cl denotes clearance.

Bio-distribution Study

Targeting efficiency of ANG conjugated dendrimeric formulations and TMZ in different organs (**Figure 10A)** were evaluated in Sprague-dawley rats. Through this study, the important objective was to evaluate the access of TMZ based nanocarriers in brain.

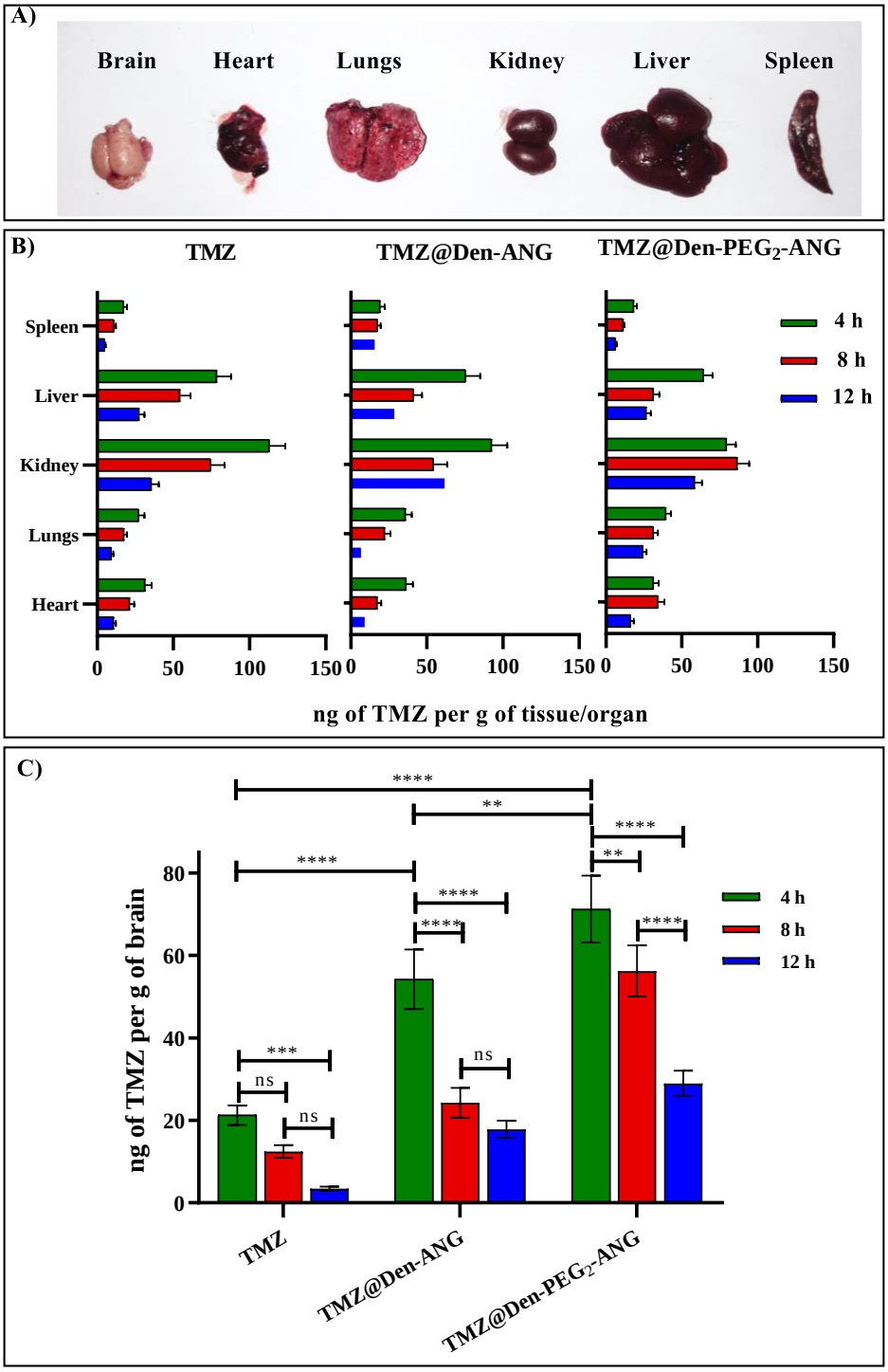

Figure 10: A) represents the vital organs analyzed through HPLC to evaluate TMZ distribution and **B)** TMZ distribution in different organs after 4, 8, and 12 h of intravenous administration of pure TMZ, TMZ@Den-ANG, and TMZ@Den-PEG$_2$-ANG to healthy Sprague-Dawley rats. **C)** Brain uptake of TMZ, TMZ@Den-ANG, and TMZ@Den-PEG$_2$-ANG at different time points. ****, ***, **, *, and ns signify $p < 0.0001$, $p = 0.0005$, $p = 0.0024$, $p = 0.0499$, and $p > 0.05$, respectively. Values represent mean ± SD (n = 4).

The outcomes suggested that pure TMZ and both the developed drug loaded formulations (TMZ@Den-ANG and TMZ@Den-PEG_2-ANG) were well taken up by liver and kidney. After 4 h of intravenous administration, the drug accumulated at kidney for pure TMZ, TMZ@Den-ANG, and TMZ@Den-PEG_2-ANG were found to be 112.94 ± 10.5, 92.46 ± 10.4, and 79.47 ± 6.2 ng per g of kidney, respectively. Surprisingly, the drug taken up by kidney was increased after 8 h in case of TMZ@Den-PEG_2-ANG. The drug distribution in lungs was maximum in case of TMZ@Den-PEG_2-ANG with drug content of 39.46 ± 3.3 ng per g of lungs and followed time dependent decline in all the treated samples. In case of heart and spleen, the drug distribution to tissues were found to be minimal as depicted in **figure 10B**.

After 4 h of administration, the brain uptake values of TMZ@Den-ANG and TMZ@Den-PEG_2-ANG were found to be 2.55 and 3.35 times higher than that of pure TMZ, respectively **(Figure 10C)**. After 12 h of administration, the brain uptake of pure TMZ was declined to less than 4 ng per g of brain tissue. The brain uptake values of TMZ@Den-ANG and TMZ@Den-PEG_2-ANG were also declined after 12 h, but remained 5.23 and 8.50 times higher than that of pure TMZ, respectively. TMZ@Den-PEG_2-ANG increased the bioavailability along with the half-life and mean residence time of the drug, which might have contributed towards the higher brain uptake.

6. STATISTICAL ANALYSIS

All the protocols were performed in triplicate. GraphPad Prism 8.0 software was utilized for the statistical analysis of the obtained outcomes through two-way ANOVA which included Tukey's multiple comparison test and Sidak's multiple comparison test. The data analysis was also performed using M.S. excel.

7. DISCUSSION

D_2O was used as solvent in case of Den-PEG_2-ANG conjugates. As depicted in **figure 4B**, the characteristic peaks were observed in the range of 2.3 to 3.0 ppm for PAMAM dendrimers and 3.5 to 4.0 ppm for PEG. The characteristic peaks of ANG structure were identified in the range of 3.0 to 4.3 ppm. These findings confirmed the synthesis of Den-PEG_2-ANG conjugates. Similar findings were observed in a previously published work [17].

The obtained parameters inferred that the surface of Den-ANG and Den-PEG_2-ANG conjugates were rough. The high and positive Skewness values represent the symmetric distribution with heavy tails. The high positive values were obtained in case of Kurtosis parameter, which indicated the presence of high-pitched peak surfaces. PEGylation of

PAMAM dendrimers might have contributed towards the reduction of surface roughness in comparison to non-PEGylated dendrimers.

PEGylation might be the reason behind the slight increment in particle size of TMZ@Den-PEG_2-ANG in comparison to the non-PEGylated formulation. The nanometric size of the formulations may result in prolonged blood circulation, which may lead to better brain permeation of the developed ANG-based formulations. The PDI values suggested the monodispersed nature of the dendrimeric nano-formulations.

PEGylated formulations showed higher entrapment efficiency and drug loading than the non-PEGylated formulations [25]. The formulation characterization resulted in similar findings, which supported the grafting of PEG molecules on to the surface PAMAM dendrimers. This might have contributed to the increase in particle size of the PEGylated formulations.

The results obtained revealed that both the peptide-functionalized formulations released TMZ in a sustained manner for 72 h. However, TMZ@Den-PEG_2-ANG showed better controlled and prolonged drug release as compared to TMZ@Den-ANG. Previously, PEGylation of PAMAM dendrimers have exhibited controlled and prolonged drug release, which has also been reported in our previous publication [25]. It also prohibits the burst drug release from the nanocarriers. Similar results were obtained in case ANG grafted PEGylated dendrimers, which supported further evaluation of the developed formulations.

In our previous publication, it was observed that PEGylation plays an important role in the enhancement of biocompatibility of the nanocarriers [25]. It masks the non-compatible amine terminal groups responsible for the lysis of RBCs. PEGylation must have reduced the hemolytic effect in comparison to the non-PEGylated formulation. The negligible hemolytic effects of the formulation promoted the *in-vitro* efficacy evaluation.

Both pure TMZ and the developed nano-formulations exhibited inhibitory effect against U87MG GBM cells. Results were similar to the findings of previous reports [26,27]. The outcome of MTT based cytotoxicity assay suggested that TMZ@Den-PEG_2-ANG imparted maximum inhibitory effect in U87MG cells. Therefore, further *in-vitro* studies were explored using U87MG cells. The increase in the treatment period significantly enhanced the cytotoxic activity with percent cell inhibition. The sustained release of TMZ from the dendrimeric formulation might be the reason for its cytotoxic effectiveness. It can be stated that the

PEGylated peptide grafted dendrimeric formulation i.e., Den-PEG_2-ANG can efficiently enhance the targeted delivery of therapeutic moieties to the glioblastoma region.

TMZ is capable of arresting the cell cycle progression at G2/M phase [28]. The outcomes of cell cycle analysis also showed similar results. The prepared dendrimeric formulations can halt the cell cycle at S-phase and G2/M phase, most effectively after 48 h of treatment. The results of MTT asaay, cellular uptake, and cell cycle analysis promoted further evaluation of the TMZ loaded nanocarriers through *in-vivo* experiments to estimate the formulation behavior in healthy animals.

In comparison other routes, intravenous administration of TMZ has shown better outcomes in terms bioavailability of the drug [29]. TMZ encapsulated dendrimer-based formulations exhibited better pharmacokinetic properties in rats than pure TMZ. The obtained pharmacokinetic parameters can be corelated with the findings of *in-vitro* drug release study. The bioavailability, half-life, and mean residence time of the developed formulations were improved as both the dendrimeric formulations namely, TMZ@Den-ANG and TMZ@Den-PEG_2-ANG showed sustained drug release behavior. The reduced clearance rate also attributed towards the enhanced circulation time of the drug. Overall, the pharmacokinetic behavior of the drug was significantly improved by the formulations, maximally by TMZ@Den-PEG_2-ANG. PEGylation plays an important role in improving the pharmacokinetic properties of the anticancer drugs, which has been also reported in our previous publication [25]. Surface modification of dendrimers might be the reason for better pharmacokinetic behavior of TMZ@Den-PEG_2-ANG.

BBB affects the brain delivery of drugs, thereby remains as a potential challenge in the treatment of GBM. ANG grafted nanocarrier have shown immense potential in brain delivery of therapeutic moieties with significant anticancer activities [30,31]. Similarly, ANG grafted dendrimers can easily cross the BBB due to the presence of LRP-1 receptors and may result in effective anticancer effects. Both the ANG grafted dendrimer-based formulations showed significant brain accumulation of TMZ. Additionally, PEGylation of dendrimers reduces the inherent toxicity aspect and might have contributed in potentiating the drug delivery across the BBB. As Den-PEG_2-ANG exhibited maximum brain permeation, it can be a potential carrier in the delivery of anticancer moieties to the brain.

8. IMPACT OF THE RESEARCH IN THE ADVANCEMENT OF KNOWLEDGE OR BENEFIT TO MANKIND

The PEGylated (Den-PEG_2-ANG) and non-PEGylated (Den-ANG) conjugates of angiopep-2 were successfully synthesized and characterized through ^1H NMR spectroscopy. The surface of Den-ANG and Den-PEG_2-ANG conjugates were observed to be rough. TMZ loaded formulations were observed to have nanometric size with excellent drug loading. FT-IR spectra also confirmed TMZ loading in the dendrimeric formulations. The ANG grafted PEGylated formulation were biocompatible in nature and showed sustained drug delivery up to 72 h. Cytotoxicity evaluation in U87MG cells revealed that TMZ@Den-PEG_2-ANG possessed significant anticancer activities with minimal IC_{50} values. The outcome of cellular uptake and cell cycle analysis also supported the findings of MTT assay. At *in-vivo* level, the pharmacokinetic properties of TMZ were improved by the PEGylated nanocarrier in terms of half-life, bioavailability, and circulation time. Organ distribution studies further ensured the enhanced brain penetration of the developed formulation. The brain delivery potential of Den-PEG_2-ANG was significantly higher than Den-ANG ($p = 0.0024$).

Targeting the brain tumor through LRP-1 receptor resulted in excellent findings at *in-vitro* and *in-vivo* level. As the brain penetration of TMZ was enhanced significantly, the therapeutic efficacy of the drug may also increase at *in-vivo* levels. PEGylation has also affected the drug permeation positively and contributed towards the biocompatibility as well as brain tissue penetration. ANG grafted PEGylated dendrimers can be a potential nanocarrier to deliver chemoitherapeutic agents to brain. However, exploration of the therapeutic efficacy of the developed formulations in brain tumor induced animals may provide more clarity.

9. REFERENCES

(1) Huang, S.; Li, J.; Han, L.; Liu, S.; Ma, H.; Huang, R.; Jiang, C. Dual Targeting Effect of Angiopep-2-Modified, DNA-Loaded Nanoparticles for Glioma. *Biomaterials* **2011**, *32* (28), 6832–6838. https://doi.org/10.1016/J.BIOMATERIALS.2011.05.064.

(2) Urbanska, K.; Sokolowska, J.; Szmidt, M.; Sysa, P. Glioblastoma Multiforme – an Overview. *Contemp. Oncol.* **2014**, *18* (5), 307. https://doi.org/10.5114/WO.2014.40559.

(3) Stark, A. M.; Maslehaty, H.; Hugo, H. H.; Mahvash, M.; Mehdorn, H. M. Glioblastoma of the Cerebellum and Brainstem. *J. Clin. Neurosci.* **2010**, *17* (10), 1248–1251. https://doi.org/10.1016/J.JOCN.2010.02.015.

(4) Cancer Today https://gco.iarc.fr/today/ (accessed Oct 15, 2022).

(5) Gutkin, A.; Cohen, Z. R.; Peer, D. Harnessing Nanomedicine for Therapeutic Intervention in Glioblastoma. *Expert Opin. Drug Deliv.* **2016**, *13* (11), 1573–1582. https://doi.org/10.1080/17425247.2016.1200557.

(6) Singh, P. K.; Singh, V. K.; Tomar, J.; Azam, A.; Gupta, S.; Kumar, S. Spinal Glioblastoma Multiforme: Unusual Cause of Post-Traumatic Tetraparesis. *J. Spinal Cord Med.* **2016**, *32* (5), 583–586. https://doi.org/10.1080/10790268.2009.11754565.

(7) Shahideh, M.; Fallah, A.; Munoz, D. G.; Loch MacDonald, R. Systematic Review of Primary Intracranial Glioblastoma Multiforme with Symptomatic Spinal Metastases, with Two Illustrative Patients. *J. Clin. Neurosci.* **2012**, *19* (8), 1080–1086. https://doi.org/10.1016/J.JOCN.2011.09.024.

(8) Qiao, C.; Yang, J.; Shen, Q.; Liu, R.; Li, Y.; Shi, Y.; Chen, J.; Shen, Y.; Xiao, Z.; Weng, J.; Zhang, X. Traceable Nanoparticles with Dual Targeting and ROS Response for RNAi-Based Immunochemotherapy of Intracranial Glioblastoma Treatment. *Adv. Mater.* **2018**, *30* (18), 1–9. https://doi.org/10.1002/adma.201705054.

(9) Shi, H.; Sun, S.; Xu, H.; Zhao, Z.; Han, Z.; Jia, J.; Wu, D.; Lu, J.; Liu, H.; Yu, R. Combined Delivery of Temozolomide and Siplk1 Using Targeted Nanoparticles to Enhance Temozolomide Sensitivity in Glioma. *Int. J. Nanomedicine* **2020**, *15*, 3347–3362. https://doi.org/10.2147/IJN.S243878.

(10) Li, K.; Liang, N.; Yang, H.; Liu, H.; Li, S. Temozolomide Encapsulated and Folic Acid Decorated Chitosan Nanoparticles for Lung Tumor Targeting: Improving Therapeutic Efficacy Both in Vitro and in Vivo. *Oncotarget* **2017**, *8* (67), 111318. https://doi.org/10.18632/ONCOTARGET.22791.

(11) Sowińska, M.; Szeliga, M.; Morawiak, M.; Zabłocka, B.; Urbanczyk-Lipkowska, Z. Design, Synthesis and Activity of New N1-Alkyl Tryptophan Functionalized Dendrimeric Peptides against Glioblastoma. *Biomolecules* **2022**, *12* (8), 1116. https://doi.org/10.3390/BIOM12081116.

(12) Fana, M.; Gallien, J.; Srinageshwar, B.; Dunbar, G. L.; Rossignol, J. PAMAM Dendrimer Nanomolecules Utilized as Drug Delivery Systems for Potential Treatment of Glioblastoma: A Systematic Review. *Int. J. Nanomedicine* **2020**, *15*, 2789–2808. https://doi.org/10.2147/IJN.S243155.

(13) Liu, Z.; Ji, X.; He, D.; Zhang, R.; Liu, Q.; Xin, T. Nanoscale Drug Delivery Systems in

Glioblastoma. *Nanoscale Res. Lett.* **2022**, *17* (1). https://doi.org/10.1186/S11671-022-03668-6.

(14) Gajbhiye, K. R.; Pawar, A.; Mahadik, K. R.; Gajbhiye, V. PEGylated Nanocarriers: A Promising Tool for Targeted Delivery to the Brain. *Colloids Surfaces B Biointerfaces* **2020**, *187*, 110770. https://doi.org/10.1016/J.COLSURFB.2019.110770.

(15) Zhang, F.; Xu, C. L.; Liu, C. M. Drug Delivery Strategies to Enhance the Permeability of the Blood–Brain Barrier for Treatment of Glioma. *Drug Des. Devel. Ther.* **2015**, *9*, 2089. https://doi.org/10.2147/DDDT.S79592.

(16) Sánchez-Navarro, M.; Giralt, E.; Teixidó, M. Blood–Brain Barrier Peptide Shuttles. *Curr. Opin. Chem. Biol.* **2017**, *38*, 134–140. https://doi.org/10.1016/J.CBPA.2017.04.019.

(17) Ke, W.; Shao, K.; Huang, R.; Han, L.; Liu, Y.; Li, J.; Kuang, Y.; Ye, L.; Lou, J.; Jiang, C. Gene Delivery Targeted to the Brain Using an Angiopep-Conjugated Polyethyleneglycol-Modified Polyamidoamine Dendrimer. *Biomaterials* **2009**, *30* (36), 6976–6985. https://doi.org/10.1016/J.BIOMATERIALS.2009.08.049.

(18) Koppu, S.; Oh, Y. J.; Edrada-Ebel, R. A.; Blatchford, D. R.; Tetley, L.; Tate, R. J.; Dufès, C. Tumor Regression after Systemic Administration of a Novel Tumor-Targeted Gene Delivery System Carrying a Therapeutic Plasmid DNA. *J. Control. Release* **2010**, *143* (2), 215–221. https://doi.org/10.1016/J.JCONREL.2009.11.015.

(19) Spyropoulos-Antonakakis, N.; Sarantopoulou, E.; Trohopoulos, P. N.; Stefi, A. L.; Kollia, Z.; Gavriil, V. E.; Bourkoula, A.; Petrou, P. S.; Kakabakos, S.; Semashko, V. V.; Nizamutdinov, A. S.; Cefalas, A. C. Selective Aggregation of PAMAM Dendrimer Nanocarriers and PAMAM/ZnPc Nanodrugs on Human Atheromatous Carotid Tissues: A Photodynamic Therapy for Atherosclerosis. *Nanoscale Res. Lett.* **2015**, *10* (1), 1–19. https://doi.org/10.1186/s11671-015-0904-5.

(20) Shen, F.; Decosterd, L. A.; Gander, M.; Leyvraz, S.; Biollaz, J.; Lejeune, F. Determination of Temozolomide in Human Plasma and Urine by High-Performance Liquid Chromatography after Solid-Phase Extraction. *J. Chromatogr. B Biomed. Sci. Appl.* **1995**, *667* (2), 291–300. https://doi.org/10.1016/0378-4347(95)00040-P.

(21) Gupta, A.; Ahmad, A.; Singh, H.; Kaur, S.; Neethu, K. M.; Ansari, M. M.; Jayamurugan, G.; Khan, R. Nanocarrier Composed of Magnetite Core Coated with Three Polymeric

Shells Mediates LCS-1 Delivery for Synthetic Lethal Therapy of BLM-Defective Colorectal Cancer Cells. *Biomacromolecules* **2018**, *19* (3), 803–815. https://doi.org/https://doi.org/10.1021/acs.biomac.7b01607.

(22) Codony-Servat, J.; Tapia, M. A.; Bosch, M.; Oliva, C.; Domingo-Domenech, J.; Mellado, B.; Rolfe, M.; Ross, J. S.; Gascon, P.; Rovira, A.; Albanell, J. Differential Cellular and Molecular Effects of Bortezomib, a Proteasome Inhibitor, in Human Breast Cancer Cells. *Mol. Cancer Ther.* **2006**, *5* (3), 665–675. https://doi.org/10.1158/1535-7163.MCT-05-0147.

(23) Mosmann, T. Rapid Colorimetric Assay for Cellular Growth and Survival: Application to Proliferation and Cytotoxicity Assays. *J. Immunol. Methods* **1983**, *65* (1–2), 55–63. https://doi.org/10.1016/0022-1759(83)90303-4.

(24) Dengler, W. A.; Schulte, J.; Berger, D. P.; Mertelsmann, R.; Fiebig, H. H. Development of a Propidium Iodide Fluorescence Assay for Proliferation and Cytotoxicity Assays. *Anticancer. Drugs* **1995**, *6* (4), 522–532. https://doi.org/10.1097/00001813-199508000-00005.

(25) Sahoo, R. K.; Gothwal, A.; Rani, S.; Nakhate, K. T.; Ajazuddin; Gupta, U. PEGylated Dendrimer Mediated Delivery of Bortezomib: Drug Conjugation versus Encapsulation. *Int. J. Pharm.* **2020**, *584*, 119389. https://doi.org/10.1016/J.IJPHARM.2020.119389.

(26) Ward, S. M.; Skinner, M.; Saha, B.; Emrick, T. Polymer-Temozolomide Conjugates as Therapeutics for Treating Glioblastoma. *Mol. Pharm.* **2018**, *15* (11), 5263–5276. https://doi.org/https://doi.org/10.1021/acs.molpharmaceut.8b00766.

(27) Banstola, A.; Duwa, R.; Emami, F.; Jeong, J. H.; Yook, S. Enhanced Caspase-Mediated Abrogation of Autophagy by Temozolomide-Loaded and Panitumumab-Conjugated Poly(Lactic- Co-Glycolic Acid) Nanoparticles in Epidermal Growth Factor Receptor Overexpressing Glioblastoma Cells. *Mol. Pharm.* **2020**, *17* (11), 4386–4400. https://doi.org/10.1021/acs.molpharmaceut.0c00856.

(28) Lan, Y.; Lou, J.; Hu, J.; Yu, Z.; Lyu, W.; Zhang, B. Downregulation of SNRPG Induces Cell Cycle Arrest and Sensitizes Human Glioblastoma Cells to Temozolomide by Targeting Myc through a P53-Dependent Signaling Pathway. *Cancer Biol. Med.* **2020**, *17* (1), 112. https://doi.org/10.20892/J.ISSN.2095-3941.2019.0164.

(29) Diez, B. D.; Statkevich, P.; Zhu, Y.; Abutarif, M. A.; Xuan, F.; Kantesaria, B.; Cutler,

D.; Cantillon, M.; Schwarz, M.; Pallotta, M. G.; Ottaviano, F. H. Evaluation of the Exposure Equivalence of Oral versus Intravenous Temozolomide. *Cancer Chemother. Pharmacol.* **2010**, *65* (4), 727. https://doi.org/10.1007/S00280-009-1078-6.

(30) Gao, H.; Zhang, S.; Cao, S.; Yang, Z.; Pang, Z.; Jiang, X. Angiopep-2 and Activatable Cell-Penetrating Peptide Dual-Functionalized Nanoparticles for Systemic Glioma-Targeting Delivery. *Mol. Pharm.* **2014**, *11* (8), 2755–2763. https://doi.org/10.1021/mp500113p.

(31) Zhu, J.; Zhang, Y.; Chen, X.; Zhang, Y.; Zhang, K.; Zheng, H.; Wei, Y.; Zheng, H.; Zhu, J.; Wu, F.; Piao, J. G.; Zhu, Z.; Li, F. Angiopep-2 Modified Lipid-Coated Mesoporous Silica Nanoparticles for Glioma Targeting Therapy Overcoming BBB. *Biochem. Biophys. Res. Commun.* **2021**, *534*, 902–907. https://doi.org/10.1016/J.BBRC.2020.10.076.